J. Fluid Mech. (1983), *vol.* 130, *pp.* 59–72
Printed in Great Britain

Perturbed bifurcation theory for Poiseuille annular flow

By GARY S. STRUMOLO
Schlumberger–Doll Research, Old Quarry Road, Ridgefield, Connecticut 06877

(Received 19 October 1981 and in revised form 15 December 1982)

The consequence of imposing an axisymmetric travelling-wave disturbance on the Poiseuille flow between two concentric cylinders is examined. A nonlinear analysis is taken, using perturbed bifurcation and singular perturbation theory, to determine how resonant wall oscillations affect flow stability. Subcritical, stable, finite-amplitude perturbations to the basic Poiseuille flow are found and conjectures on their significance are given.

1. Introduction

In this section we give a description of the basic problem and describe the equations of motion. Section 2 outlines the linear stability theory for the Poiseuille motion that leads to an Orr–Sommerfeld-like system of equations for the disturbance stream function. The formal perturbation expansions to determine the bifurcation solutions are also noted. These are evaluated numerically since they constitute the lowest-order terms in our subsequent work. Section 3 describes the perturbed bifurcation analysis to examine the effect that imposing a travelling-wave disturbance to the outer cylinder will have on the stability of the Poiseuille flow. Inner and outer expansions (about the critical Reynolds number R_c) are formally derived for this singular perturbation problem and the effects of resonant oscillations are examined. Section 4 analyses the amplitude equation for the inner expansion and shows how the response curve (relating disturbance amplitude to Reynolds number) varies with the rate of change of the wall temporal oscillation with respect to the Reynolds number. Section 5 examines the stability of the response curves as the radius ratio η approaches unity (channel flow). Section 6 presents a general discussion of the results along with its limitations.

1.1. *Problem description*

The basic problem consists of the motion of a viscous, incompressible, single-phase fluid enclosed between two concentric cylinders. The motion of the fluid is produced by a fixed axial pressure gradient (see figure 1). Equations describing this flow are derived from the Navier–Stokes equations. Our analysis in this paper will be restricted to axisymmetric motions and disturbances. Under these conditions we may introduce a stream function ψ such that

$$V_x = \frac{1}{r}\frac{\partial \tilde{\tilde{\psi}}}{\partial r}, \quad V_r = -\frac{1}{r}\frac{\partial \tilde{\tilde{\psi}}}{\partial x}. \tag{1.1}$$

We may resolve this motion into Poiseuille annular flow $\tilde{\psi}$ plus a disturbance ψ',

$$\tilde{\tilde{\psi}} = \tilde{\psi} + \psi', \quad \frac{\partial \tilde{\psi}}{\partial r} = rU_x, \tag{1.2}$$

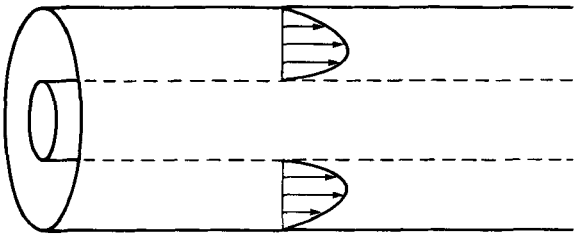

FIGURE 1. Concentric cylinders for annular Poiseuille flow; inner radius r_1, outer radius r_2.

where

$$U_x = 2\langle U_x\rangle \frac{r_2^2 - r^2 - 2r_m^2 \ln(r_2/r)}{r_2^2 + r_1^2 - 2r_m^2}, \tag{1.3}$$

$$r_m^2 = (r_1^2 - r_2^2)/2\ln\eta, \quad \eta = r_1/r_2$$

and $\langle U_x\rangle$ is the average velocity.† With this decomposition, we are led to the following nonlinear boundary-value problem for the disturbance stream function:

$$\left.\begin{aligned} &\frac{\partial}{\partial t}\mathrm{D}^2\psi' + U_x\frac{\partial}{\partial x}\mathrm{D}^2\psi' - r\frac{\mathrm{d}}{\mathrm{d}r}\frac{1}{r}\frac{\mathrm{d}U_x}{\mathrm{d}r}\frac{\partial}{\partial x}\psi' + J(\psi', \mathrm{D}^2\psi') = \nu\,\mathrm{D}^4\psi', \\ &\psi' = \frac{\partial\psi'}{\partial r} = 0 \quad \text{at} \quad r = r_1, r_2, \\ &\mathrm{D}^2 = \frac{\partial^2}{\partial r^2} - \frac{1}{r}\frac{\partial}{\partial r} + \frac{\partial^2}{\partial x^2}, \\ &J(\psi', \mathrm{D}^2\psi') = \frac{1}{r}\left(\frac{\partial\psi'}{\partial r}\frac{\partial}{\partial x}\mathrm{D}^2\psi' - \frac{\partial\psi'}{\partial x}\frac{\partial}{\partial r}\mathrm{D}^2\psi'\right) + \frac{2}{r}\frac{\partial\psi'}{\partial x}\mathrm{D}^2\psi'. \end{aligned}\right\} \tag{1.4}$$

We can make the problem nondimensional by introducting the values $L = \frac{1}{2}(r_2 - r_1)$ and $\langle U_x\rangle$ as the characteristic length and velocity respectively for the flow. We then have

$$a \equiv \frac{2\eta}{1-\eta} \leqslant r \leqslant \frac{2}{1-\eta} \equiv b, \quad -\infty < x < \infty, \tag{1.5}$$

and the Reynolds number

$$R = \langle U_x\rangle L/\nu.$$

From this point on, we will deal with dimensionless quantities only.

2. Linear stability and bifurcation theory

Let us write $\psi' = \epsilon\psi$, where ϵ is a small parameter measuring the amplitude of the disturbance. If we insert this into the dimensionless version of (1.4) and linearize in ϵ, we arrive at the spectral problem for the instability of annular flow. In particular, we are led to an Orr–Sommerfeld-like system

$$\left(U - \frac{\omega}{\alpha}\right)\left(\phi'' - \frac{1}{r}\phi' - \alpha^2\phi\right) - \left(U'' - \frac{1}{r}U'\right)\phi = \frac{\lambda}{\mathrm{i}\alpha}\left[\phi^{\mathrm{iv}} - \frac{2}{r}\phi''' + \left(\frac{3}{r_2} - 2\alpha^2\right)\left(\phi'' - \frac{1}{r}\phi\right) + \alpha^4\delta\right], \tag{2.1}$$

$$\phi = \phi' = 0 \quad \text{at} \quad r = a, b,$$

† This research was motivated by the problems encountered in the logging of wellbores in oil-producing reservoirs. The range $0.183 \leqslant \eta \leqslant 0.644$ is characteristic for this area and this interval is depicted on a number of subsequent figures.

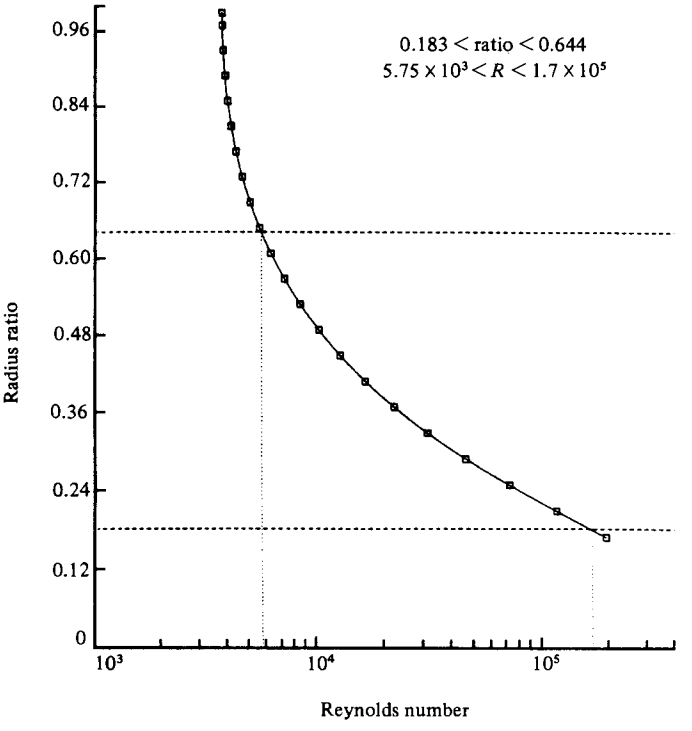

FIGURE 2. Plot of critical numbers R_c for a range of η-values – linear stability theory.

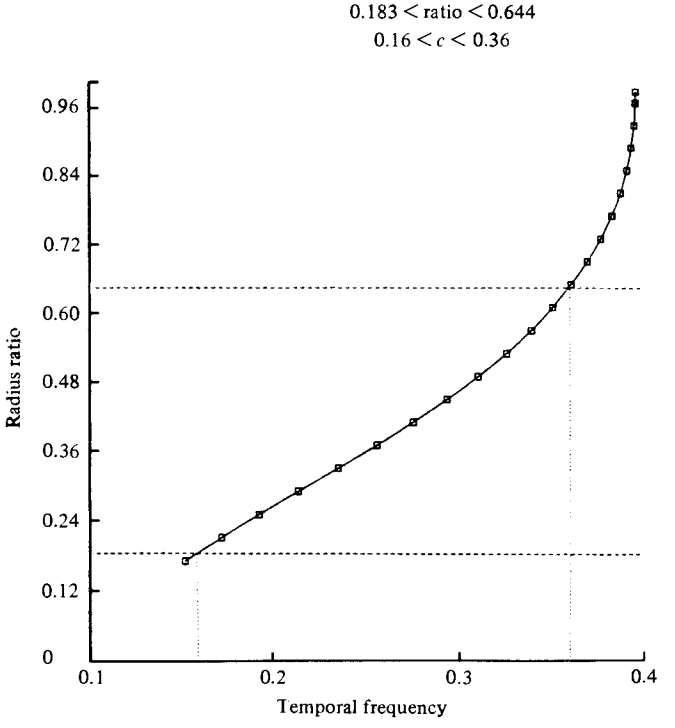

FIGURE 3. Plot of temporal frequency at criticality *vs.* η.

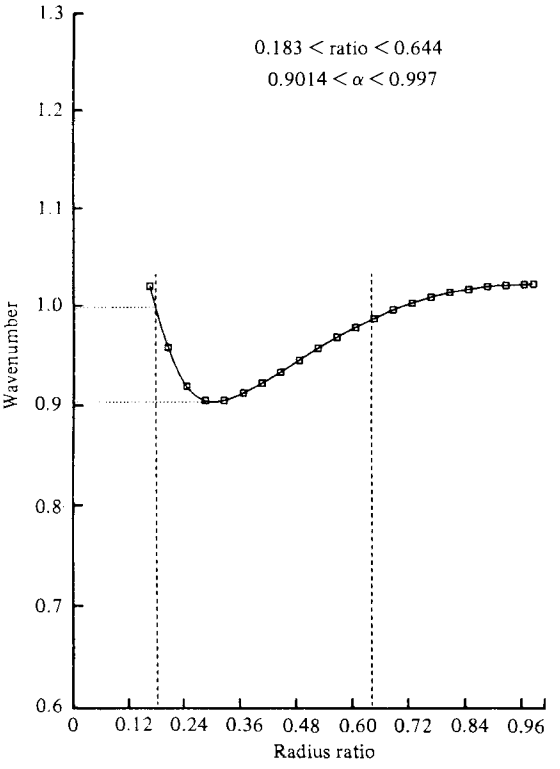

FIGURE 4. Plot of critical wavenumber *vs.* η.

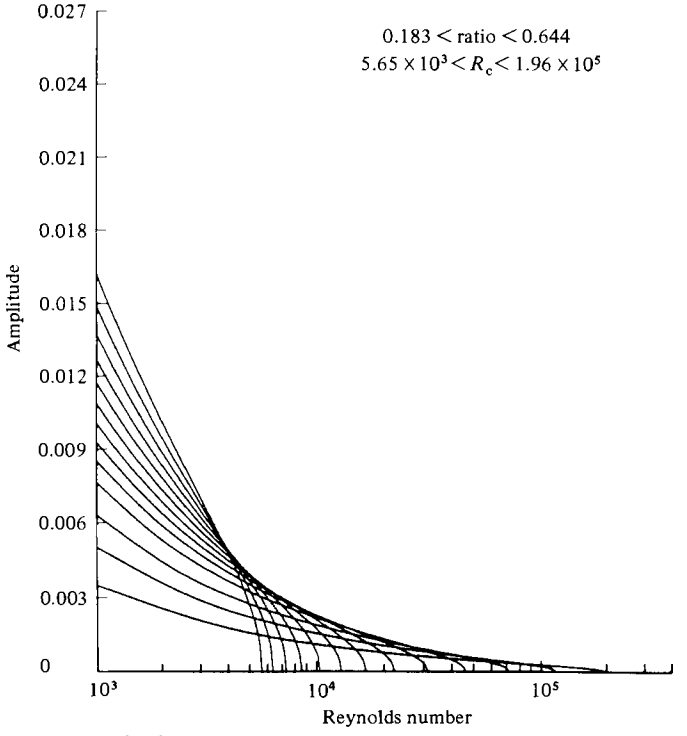

FIGURE 5. (R, ϵ)-plot of bifurcation curves using $\lambda = \lambda_c + \epsilon^2\lambda_2$ from (2.3), η-range as indicated. Each curve corresponds to a different η-value. The intercept on the R-axis is the value of R_c for that particular η.

where we have written $U = U_x/\langle U_x \rangle$, $\lambda = 1/R$ and

$$\psi = \mathrm{e}^{-\gamma(\lambda)t}\, \mathrm{e}^{\mathrm{i}\alpha x}\, \phi(r,\lambda). \tag{2.2}$$

For any point in the (α, R)-plane the eigenvalue γ is generally complex. If its real part is positive, the disturbance will decay exponentially in time and the basic (Poiseuille) state is said to be stable. If its real part is negative, the disturbance will grow in time and give rise to instability. When the eigenvalue is purely imaginary, $\gamma = \mathrm{i}\omega$, we have neutral stability. The locus of points in the (α, R)-plane for which a corresponding eigenvalue is purely imaginary is called the neutral curve for that eigenvalue; it separates stable and unstable regions. R_c, the least R for which an eigenvalue of the spectral problem has a purely imaginary value, is called the critical Reynolds number for the flow. Using a new continuation procedure,† this system has been solved for a range of η-values. A plot of the critical Reynolds numbers for the linear stability theory is given in figure 2. Plots of the temporal frequency and wavenumber at the critical points are given in figures 3 and 4. All of these results on linear stability have been derived before. In addition, Joseph & Chen (1974) showed that a branch of solutions, periodic in both space and time, bifurcate subcritically from the laminar flow solution U at $R = R_c$. The bifurcation curves for these η values are depicted in figure 5. Floquet analysis (where we examine the stability of perturbations about these states) can be used to demonstrate that these subcritical bifurcating solutions (amplitude decreasing with increasing R) are unstable. We can compute these solutions by seeking them in the form of a perturbation series about the basic state:

$$\begin{bmatrix} \psi \\ \lambda \\ \omega \end{bmatrix} = \sum_{l=0}^{\infty} \epsilon^l \begin{bmatrix} \psi_l \\ \lambda_l \\ \omega_l \end{bmatrix}, \quad \lambda_0 = \lambda_c, \tag{2.3}$$

where the zeroth-order terms correspond to the critical eigenvalues and eigenfunctions at R_c. These calculations were carried out and agree well with those reported by Joseph and Chen (1974). They constitute the lowest-order terms for § 3.

3. Perturbed bifurcation analysis

We shall analyse our problem using the methods of Matkowsky & Reiss (1977) and Reiss (1977), where the general theory of singular perturbations of bifurcations is described. For a discussion on nonlinear effects in (plane) Poiseuille flow, see Meksyn & Stuart (1951), Stuart (1960), Watson (1960), Pekeris & Shkoller (1967), Reynolds & Potter (1967) and Stewartson & Stuart (1971). Of course this list is by no means exhaustive; for a more extensive bibliography on the subject of fluid stability, see Joseph (1976).

3.1. *Outer expansions*

We now consider what effect a small 'imperfection' on the shape of the outer cylinder will have on the stability of the flow. We impose a sinusoidal radius variation as illustrated in figure 6 of amplitude $\delta \ll 1$. The differential equation (1.4) for ψ' remains as before, but the boundary conditions change, leading to the new system (we

† The details of this procedure are contained in an appendix that has been lodged in the editorial files. Copies may be obtained from the editor or the author on request.

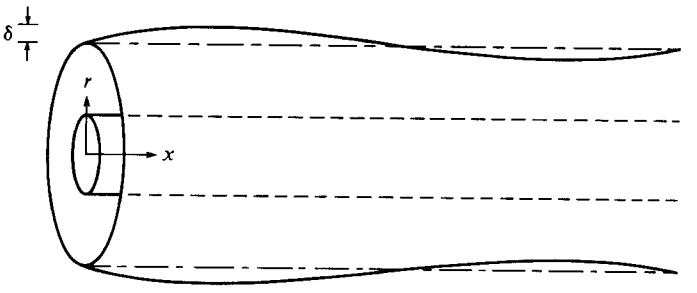

Outer wall: $r = b + \delta F(x, t)$

$F(x, t) = \frac{1}{2}(e^{i(\alpha x - ct)} + e^{-i(\alpha x - ct)})$

$c = c(\lambda) = w_0 + w_1(\lambda - \lambda c) + w_2(\lambda - \lambda c)^2 + \ldots$

FIGURE 6. Travelling-wave disturbance imposed on outer cylinder with amplitude δ. Temporal frequency c is real and a function of the Reynolds number.

hereinafter drop the prime convention):

$$\left.\begin{aligned} \psi_r = \psi_x = 0 \quad &\text{at} \quad r = a, \\ \psi_x = -r_T\,\delta F_t(x,t) \quad &\text{at} \quad r = r_T \equiv b + \delta F(x,t), \\ \psi_r = -2r_T \frac{b^2 - r_T^2 - 2r_m^2 \ln(b/r_T)}{b^2 + a^2 - 2r_m^2} \quad &\text{at} \quad r = r_T, \end{aligned}\right\} \tag{3.1}$$

and the differential equation

$$L\psi + J(\psi, D^2\psi) = 0, \tag{3.2}$$

where

$$L = L[U, \lambda] = \frac{\partial}{\partial t} D^2 + U\frac{\partial}{\partial x} D^2 - r\frac{d}{dr}\frac{1}{r}\frac{dU}{dr}\frac{\partial}{\partial x} - \lambda D^4. \tag{3.3}$$

In addition, we impose the condition that ψ along with its derivatives with respect to x remain bounded as x approaches infinity. Since δ alters (1.4) through the boundary conditions, we seek an asymptotic expansion of the solution in the form

$$\psi(x, r, t; \delta, R) = \sum_{j=0}^{\infty} \psi_j(x, r, t; R)\,\delta^j. \tag{3.4}$$

If we perturb about the basic state ($\psi_0 = 0$), insert (3.4) into the above set of equations, and equate like powers of δ, we are led to a series of linear differential equations for the ψ_j. In particular, the expression for ψ_1, using the completeness of the O–S eigenfunctions ϕ_1^ν, along with their orthogonality relationships, can be expressed in the form

$$\psi_1 = \sum_{\nu=1}^{\infty} \left\{ b_\nu\, e^{i(\alpha x - ct)}\, \phi_1^\nu(r) + \bar{b}_\nu\, e^{-i(\alpha x - ct)}\, \bar{\phi}_1^\nu(r) \right\} - h_1, \tag{3.5}$$

where

$$b_\nu(\alpha, \lambda) = \frac{g_\nu(\alpha, \lambda)}{\gamma^\nu(\alpha, \lambda) - ic(\lambda)}$$

$$g_\nu(\alpha, \lambda) = \frac{a}{2\pi^2}(b^2 - a^2) \int_0^{2\pi} \int_0^{2\pi/\alpha} \int_a^b \tilde{h}\, e^{-i(\alpha x - \tau)}\, \bar{\phi}_1^{*\nu}(r, \lambda)\, \rho\, dr\, dx\, d\tau,$$

$$\tau = ct,$$

and where h_1 and $\tilde{h}$ are derived using the Taylor expansion of ψ about $r = b$ in the boundary conditions (here $*$ denotes adjoint). In the general case, the spatial and temporal frequencies of F have no relation to those of the bifurcation solution. As a result, bifurcation is preserved and is either delayed or hastened slightly. These new bifurcating solutions are sometimes quasiperiodic in both space and time (for details on plane Poiseuille case see Strumolo 1978).

In this paper, we will consider the resonance case for our imperfection, setting the wavenumber α of F equal to the wavenumber α_0 of the critical eigenfunction. We also set the real temporal frequency of oscillation $c(\lambda)$ at lowest order equal to that of the eigenfunction, i.e. $w_0 = \omega_0$. Then since

$$\gamma^1(\alpha_0, \lambda_c) = i\omega_0, \quad c(\lambda_c) = w_0 = \omega_0, \tag{3.6}$$

we have

$$|b_1| \to \infty \quad \text{as} \quad \lambda \to \lambda_c \quad \text{provided} \quad g_1(\alpha_0, \lambda_c) \neq 0.$$

This inadmissible singularity leads us to consider an inner expansion for the region $\lambda - \lambda_c$ small in §3.2 below. Allowing c to depend upon λ (or equivalently R) enables us to consider the effects of altering dynamically the temporal frequency of the wall oscillations with the flow speed. Another interesting case would be to examine the effects of setting α near α_0, but this was not done here.

3.2. *Inner expansions*

The value of $g_1(\alpha_0, \lambda_c)$ can be shown to be non-zero inour resonance case; hence the outer expansion (3.4) is not valid in a neighborhood of λ_c. This is typical of such singular perturbation problems. To obtain a valid asymptotic expansion we must first 'stretch' the neighbourhood of λ_c by the transformation

$$\lambda = \lambda_c + \xi\mu^m + \sum_{j=2}^{\infty} \xi_j \frac{\mu^{jm}}{j!} \quad (m > 0), \tag{3.7}$$

$$\delta(\mu) = \mu^n,$$

where ξ is the stretched variable in the method of matched asymptotic expansions and $\xi_j = \xi_j(\xi)$. The constant n must be positive since we require $\delta(0) = 0$. The constants m and n must also be integers since we require that the derivatives of λ and δ with respect to μ be bounded as μ approaches zero. Since $c = c(\lambda)$, we also have

$$c = \omega_0 + w_1 \xi\mu^m + \text{higher-order terms.} \tag{3.8}$$

We look for a solution in the form

$$\psi(x, r, s; \lambda(\mu), \delta(\mu)) = Z(x, r, s; \mu) = \sum_{j=1}^{\infty} z_j(x, r, s)\mu^j, \tag{3.9}$$

where $s = ct$. Inserting this series into (3.1)–(3.3) for ψ and equating like powers of μ leads us to an equation for z_1 of the form

$$L_0 \tilde{z}_1 = \delta_\mu^0 \tilde{h}, \tag{3.10}$$

$$\tilde{z}_1 = \tilde{z}_{1r} = 0 \quad \text{at} \quad r = a, b,$$

where

$$z_1 = \tilde{z}_1 - \delta_\mu^0 h_1,$$

$$L_0 = \omega_0 \frac{\partial}{\partial s} D^2 + U \frac{\partial}{\partial x} D^2 - r \frac{d}{dr} \frac{1}{r} \frac{dU}{dr} \frac{\partial}{\partial x} - \lambda_c D^4,$$

$$\delta_\mu^0 = \frac{d}{d\mu}(\delta)\Big|_{\mu=0}.$$

Because the inner expansion is intended to be the continuation of the outer expansion in the neighbourhood of λ_c, we consider solutions z_j that have the same periodicity as those of the outer expansion. Since there are non-trivial solutions to the homogeneous version of (3.10), the Fredholm alternative theorem implies that (3.10) will have a solution if and only if the inhomogeneous term is orthogonal to the null space of the homogeneous adjoint operator. This solvability condition leads to

$$\delta_\mu^0[\hat{h}, z^*] = 0, \tag{3.11}$$

where

$$z^* = e^{i\theta}\phi_0^*(r), \quad \theta = \alpha_0 x - s,$$

$$[\hat{a}, \hat{b}] = \frac{\alpha_0}{2\pi^2(b^2-a^2)} \int_0^{2\pi} \int_0^{2\pi/\alpha_0} \int_a^b \hat{a}\hat{b} r \, dr \, dx \, ds.$$

Here $\phi_0^*(r)$ is the adjoint O–S eigenfunction at criticality. Numerical computations give a non-zero inner product, yielding

$$\delta_\mu^0 = 0, \tag{3.12}$$

$$z_1 = 2 \operatorname{Re}(A e^{i\theta}\phi_0(r)).$$

We determine the complex amplitude A by applying the solvability condition to the inhomogeneous terms of the successive higher-order problems. We impose the additional conditions that A depend upon all of the parameters and remain finite at $\lambda = \lambda_c$. This results in the following equation for A:

$$A^2\bar{A} + C_3 \xi A + C_4 = 0. \tag{3.13}$$

We will refer to this as the amplitude equation. The complex quantity C_3 is a linear function of $w_1 = c'(\lambda_c)$. The coefficients in these functions are evaluated numerically from integrals involving the Orr-Sommerfeld eigenfunction and its adjoint. We also find

$$\delta_{\mu\mu\mu}^0 \neq 0, \quad \lambda_{\mu\mu}^0 \neq 0, \quad c_{\mu\mu}^0 \neq 0, \tag{3.14}$$

and so

$$\lambda = \lambda_c + \xi\delta_3^2 + \sum_{j=2}^{\infty} \xi_j \frac{\delta_3^{2j}}{j!}. \tag{3.15}$$

Matching conditions of the method of matched asymptotic expansions could then be employed to determine how the inner and outer expansions 'connect'. Composite expansions would then give the uniform asymptotic expansions of the solution to this perturbed problem (see Strumolo & Reiss, 1981).

By using a totally different method of analysis, Hall (1978) analysed the problem of the effect of external resonant forcing on the stability of plane Poiseuille (channel) flow. Our results for the limiting case as η approaches unity agree well with his, which gives an equation similar to (3.15).

4. Analysis of the amplitude equation

With some elementary algebraic manipulations, the amplitude equation reduces to

$$\rho^3 + \beta_1\rho = \pm(\gamma^2 - \beta_2^2 r^2)^{\frac{1}{2}}, \tag{4.1}$$

where ρ is the modulus of the complex amplitude A, and the quantities β_1 and β_2 are linear functions of w_1 and ξ. We solve this equation for ξ, with solutions

$$\xi = \xi_\pm(\rho) = a\rho^2 \pm \Gamma\rho^{-\frac{1}{2}}(1-\beta\rho^6)^{\frac{1}{2}}, \tag{4.2}$$

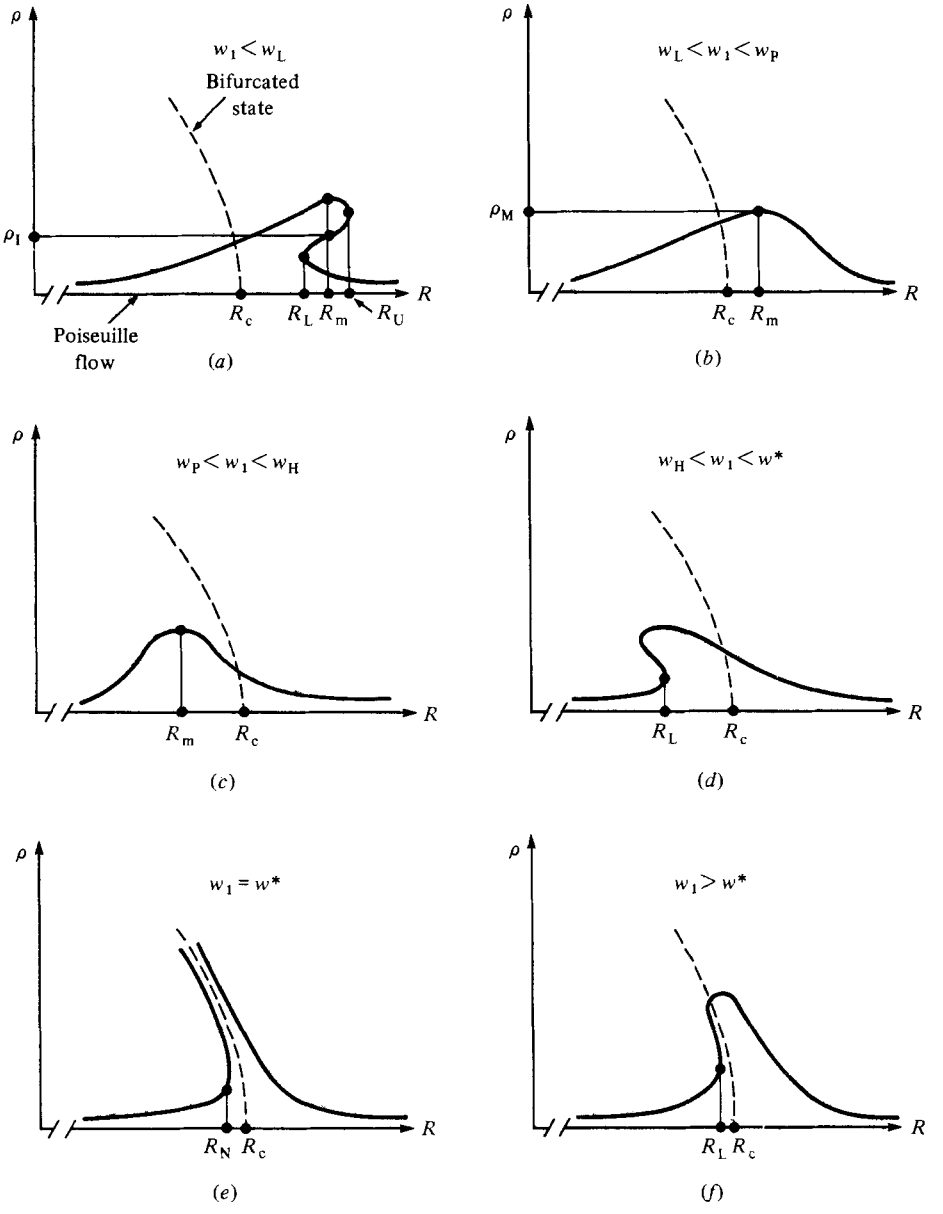

FIGURE 7. Response states when outer cylinder resonates with critical frequencies and wavenumbers at R_c. Dependence on $w_1 = c'(\lambda_c)$, the rate of change of the forced temporal oscillation with λ.

where a, β, and Γ are defined by

$$\left.\begin{aligned} a &= -\frac{p}{p^2+q^2}, \\ \beta &= \frac{(q/\gamma)^2}{p^2+q^2} > 0, \\ \Gamma &= \gamma(p^2+q^2)^{-\frac{1}{2}} > 0, \\ \beta_1 &= \xi p, \quad \beta_2 = \xi q, \quad \gamma = |C_4|. \end{aligned}\right\} \tag{4.3}$$

The values $\xi_{\pm}$, along with (3.15), give the two R-values at which a line of constant ρ would intersect the response curves in figure 7. It follows directly from (4.2) that the real roots are bounded above by

$$\rho = \rho_{\mathrm{m}} = \beta^{-\frac{1}{6}}. \tag{4.4}$$

The value of ξ corresponding to ρ_{m} is obtained from (4.2) as

$$\xi = \xi_{\mathrm{m}} = a\beta^{-\frac{1}{3}}. \tag{4.5}$$

The point $(\xi_{\mathrm{m}}, \rho_{\mathrm{m}})$ is the maximum of the response curve defined by (4.2). The position of this maximum clearly depends upon w_1, since a and β do. The value of the Reynolds number at this maximum is given by

$$\frac{1}{R_{\mathrm{m}}} = \lambda_{\mathrm{m}} = \lambda_{\mathrm{c}} + \xi_{\mathrm{m}}\,\delta^{\frac{2}{3}} + O(\delta^{\frac{4}{3}}). \tag{4.6}$$

An elementary analysis, which we do not present here (see Strumolo 1978), shows that there are four critical values of w_1, denoted by w_{L}, w_{P}, w_{H}, and w^*. The value of w_1, however, is at our disposal and this simple allowance yields the varied response curves in figure 7. For w_1 in the interval $(w_{\mathrm{L}}, w_{\mathrm{H}})$, the response curve gives the amplitude as a single-valued function of R; for w_1 outside this interval, the response curves are multivalued. The significance of the critical value w_{P} is that $R_{\mathrm{m}} > R_{\mathrm{c}}$ $(< R_{\mathrm{c}})$ if $w_1 < w_{\mathrm{P}}$ $(> w_{\mathrm{P}})$. At $w_1 = w_{\mathrm{P}}$, R_{m} and R_{c} coincide. In the case of complete resonance, i.e. when the wavenumber and temporal frequency of the imperfection function F coincide with those of the bifurcation solution, we have $w_1 = w^* = \omega_2/\lambda_2$.

The multivalued response curves define two critical values of R: R_{U} and R_{L}. They correspond respectively to the locations of the upper and lower limit points or 'noses.' Their significance will be analysed in §5. The locations of the limit points are determined by solving the equations

$$\rho^3 + \beta_1\rho = \pm(\gamma^2 - \rho^2\beta_2^2)^{\frac{1}{2}}, \tag{4.7}$$

$$3\rho^2 + \beta_1 = \mp\frac{\beta_2^2\rho}{(\gamma^2 - \rho^2\beta_2^2)^{\frac{1}{2}}}. \tag{4.8}$$

This leads to

$$3\sigma^2 + 4\beta_1\sigma + (\beta_1^2 + \beta_2^2) = 0, \quad \sigma = \mathrm{p}^2 \tag{4.9}$$

with the solutions

$$\sigma_{\pm} = \tfrac{1}{3}[-2\beta_1 \pm (\beta_1^2 - 3\beta_2^2)^{\frac{1}{2}}], \quad \rho_{\pm} = \sigma_{\pm}^{\frac{1}{2}}. \tag{4.10}$$

The two noses are then determined by inserting these values into (4.1), solving for their corresponding ξ-values, and using these values in (3.15). The locations of R_{N} (figure 7*e*) in the complete resonance case, for a range of δ and η values, are given in figure 9 along with the R_{c} values of linear stability theory.

5. Solution-branch stability analysis

Let us rewrite the amplitude equation in its original form

$$e_1 A^2\bar{A} - (\xi R_{\mathrm{c}})\, d_1 A + f_1 = 0,$$

where the coefficient d_1 is a function of w_1. Figure 7 has provided the response curves for the different ranges of w_1. We need, however, to determine the stability of these

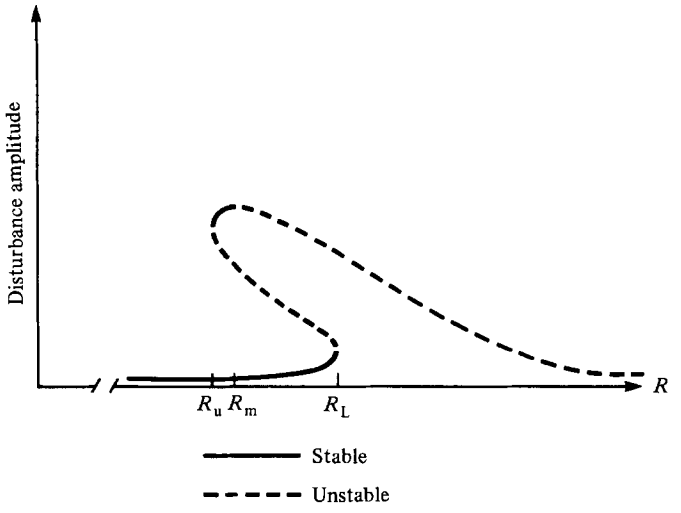

FIGURE 8. Sample response curve illustrating stable and unstable sections.

solution branches to small perturbations. By means of Floquet theory, we can easily show that, if a disturbance B of the form $B \propto e^{\lambda t}$ is added to the amplitude A, the exponent λ is given by

$$\lambda_{\pm} = (-\xi R_c)\, d_{1r} + 2|A|^2\, e_{1r} \pm [e_1\, A^2|^2 - \{(-\xi R_c)\, d_{1i} + 2|A|^2\, e_{1i}\}^2]^{\frac{1}{2}},$$

where the subscripts r and i denote the real and imaginary parts respectively. The stability of the branch is then determined by the values of λ_+ and λ_-. For example, if $\lambda_- = \mu < 0$ and $\lambda_+ = \lambda > 0$, we have a saddle point. If $\lambda_{\pm} = \alpha \pm i\beta$, then we have a focus; stable if $\alpha < 0$ and unstable if $\alpha > 0$. The values of $\lambda_{\pm}$ for different w_1 values were computed in the limiting case as η approached unity. Let us consider the cases (*d*) and (*e*) in figure 7. For w_1 near w_H, we find that the lower branch is a stable focus up to the lower limit point (nose), the middle branch is an unstable saddle point, while the upper branch changes from a stable focus (or node) to a centre to an unstable focus as R increases. Figure 8 depicts this for a particular w_1 value. As w_1 approaches w^*, the upper branch becomes completely unstable. Hence there is a lower bound on the Reynolds number R_U below which only one stable branch (near the laminar state) exists and above which two stable branches can exist. For the case $\eta = 1$, we find, for example, that, when w_1 equals 420, a stable section on the upper branch begins at

$$R_U = R_c[1 - 56.15\delta^{\frac{2}{3}} + \ldots],$$

the centre occurs at

$$R = R_c[1 - 55.18\delta^{\frac{2}{3}} + \ldots],$$

with the upper branch unstable thereafter. The maximum point occurs at

$$R_m = R_c[1 - 54.72\delta^{\frac{2}{3}} + \ldots].$$

When w_1 equals 500 ($w^* = 584$), no portion of the upper branch is stable. In the case $w_1 = w^*$, the lower branch is a stable focus up to the limit point (nose), while the other two branches are unstable.

Case (*f*) is interesting. A stability analysis here shows that, if w_1 is sufficiently large ($w_1 > 36000$ in the case $\eta = 1$), then the branch to the right of R_c is stable for all R! How we get to this branch, of course, is another matter.

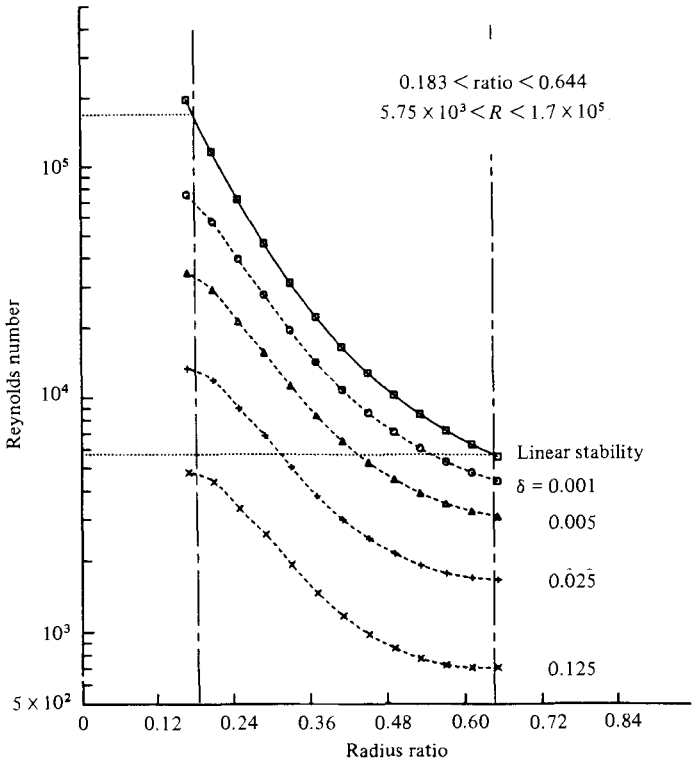

FIGURE 9. Plots of critical Reynolds numbers. Solid curve is from linear stability theory. Additional curves correspond to R_N (see figure 7*e*) for various δ-values.

6. Discussion of the results

Figure 2 depicts the critical Reynolds numbers of the linear stability theory as a function of the radius ratio η. As η decreases, R_c increases. This might be expected, since pipe flow is unconditionally stable to infinitesimal axisymmetric disturbances. The limit as η approaches zero, however, is not quite pipe flow since the no-slip condition must be satisfied at the inner cylinder regardless of its size. Such a limit could be approached by moving the inner cylinder with a velocity necessary to maintain the parabolic profile, but that analysis was beyond the scope of the present paper.

In actual experiments on channel, pipe or annular flow, however, transition takes place at Reynolds numbers much lower than those predicted by the linear theory, and a nonlinear analysis must be taken, as in this paper. Consider the cases (*d*)–(*f*) in figure 7. Under our results on the stability of the solution branches,† we find that there may be two stable sections: one small-amplitude branch for $R < R_L$, and one large-amplitude branch for $R_U < R$. These two stable branches are separated by an unstable branch for $R_U < R < R_L$, while the upper stable branch loses its stability as R increases (see figure 8 for a characteristic response curve). Of course, there is a continuum of response curves for the range of w_1 values. Two points, however, stand out: the interval (R_m, R_L) lies well below R_c, even for a small δ-value (see (3.15)),

† While §5 reported on the stability calculations for $\eta = 1$, the results are characteristic for any other radius ratio as well.

and there are two classes of stable branches – one small-amplitude and one large-amplitude. Since these are magnitudes for the disturbance stream function, the analysis indicates that two possible states can exist in this range: one near the Poiseuille state, and the other further from the Poiseuille state and of a higher amplitude.

Let us conjecture, then, what might happen according to our results as the Reynolds number is slowly increased. For small R, the flow remains approximately Poiseuille (on the lower stable branch). As R increases, there could exist a cycling between two stable states: one nearly Poiseuille and the other periodic and of higher amplitude, due to additional small-scale perturbations present in the system. Finally, the laminar state completely loses its stability and is replaced by some higher amplitude state. This is not the first time that a hypothesis of 'cycling in phase space between two distinct relatively stable but weakly attracting solutions' has been proposed (see Joseph 1976; Wyganski & Champagne 1973). However, I am unaware of any formal demonstration of their existence for these flows until now.

This cycling behaviour is similar to what is observed experimentally (Lessen & Huang 1976; Subbotin 1978; Wygnanski & Champagne 1973). Initially we have a laminar state. As R increases, sporadic bursts occur, with the flow oscillating from a laminar state to a 'turbulent' state and back again. As R increases further, the laminar state is eventually replaced by a turbulent one.

Of course, these bursts are not axisymmetric in nature, and so we cannot conclude that the cycling states we derive theoretically are those observed experimentally. An additional limitation of an axisymmetric analysis is that it excludes modes which may be even more unstable e.g. in pipe flow the most energetic initial disturbance is a spiral mode with azimuthal periodicity (Joseph 1976).

However, the assumption of resonant oscillations in an actual experiment may not be as unrealistic as one might first think. Karnitz *et al.* (1974) noted that the walls of their channel were not perfectly flat (as is assumed in a mathematical analysis). In addition, they observed that, prior to transition, periodic disturbances with the frequency and wavenumber of the Tollmien–Schlichting waves appeared at the walls. These are exactly the frequencies and wavenumbers that I consider to exist there at criticality. Finally, the allowance for the forced oscillation frequency c to vary with the Reynolds number could be made more palatable from an experimental standpoint when one realizes that altering the fluid speed will alter the vibrational characteristics of the machine used to drive it.

A final example illustrating how such travelling-wave disturbances could exist comes from the logging of oil wells. Let us consider a two-phase system consisting of a liquid and a gas flowing together in a pipe. To measure the flow rates in such a system, a cylindrical tool is placed concentrically in the pipe. Depending upon the velocities of the two phases, different flow regime patterns can arise. In one such pattern, the liquid forms a thin film around the wall of the pipe with the gas composing the central core. This regime is called annular flow.† In this case, axisymmetric travelling waves form on the liquid film and propagate up the pipe. Treating the gas as the single phase of interest, we can examine its stability to wall motions, where the liquid waves constitute the outer wall. Thus wave motions of the type discussed in this paper are physically realizable.

What, then, has our axisymmetric analysis shown? When there are no

† The term 'annular flow' in two-phase-flow jargon refers to the annular configuration of the liquid in the pipe, and not to the fact that the flow is between two concentric cylinders.

perturbations on the outer cylinder, we know that the only stable solution up to R_c is the Poiseuille state; the subcritical bifurcating solutions are unstable. With a resonant perturbation imposed, we have shown that the stability picture is significantly altered. If the temporal oscillation is dynamically adjusted with the Reynolds number as in figures 7 (*d*, *e*), we arrive at a possible 'laminar–cycling–high-amplitude' transition. It is even possible mathematically to oscillate the outer cylinder to achieve a stable solution for Reynolds numbers greater than R_c, although this may not be possible in a real experiment.

REFERENCES

HALL, P. 1978 The effect of external forcing on the stability of plane Poiseuille flow. *Proc. R. Soc. Lond.* **A359**, 453.

JOSEPH, D. D. 1976 *Stability of Fluid Motions.* Springer.

JOSEPH, D. D. & CHEN, T. S. 1974 Friction factors in the theory of bifurcating Poiseuille flow through annular ducts. *J. Fluid Mech.* **66**, 189.

KARNITZ, M. A. *et al.* 1974 An experimental investigation of transition of a plane Poiseuille flow. *Trans. A.S.M.E.* 384.

KELLER, H. B. & CEBECI, T. Numerical methods for the Orr–Sommerfeld equation. (Unpublished.)

LESSEN, M. & HUANG, P. 1976 Poiseuille flow in a pipe with axially symmetric wavy walls. *Phys. Fluids* **19**, 945.

MATKOWSKY, B. J. & REISS, E. L. 1977 Singular perturbations of bifurcations. *SIAM J. Appl. Maths* **33**, 230.

MEKSYN, D. & STUART, J. T. 1951 Stability of viscous motion between parallel planes for finite disturbance. *Proc. R. Soc. Lond.* **A208**, 517.

ORSZAG, S. A. 1971 Accurate solution of the Orr–Sommerfeld stability equation. *J. Fluid Mech.* **50**, 689.

PEKERIS, C. & SHKOLLER, B. 1967 Stability of plane Poiseuille flow to periodic disturbances of finite amplitude in the vicinity of the neutral curve. *J. Fluid Mech.* **29**, 31.

REISS, E. L. 1977 Imperfect bifurcation. *Advanced Seminar on Bifurcation Theory.* Univ. of Wisconsin.

REYNOLDS, W. C. & POTTER, M. C. 1967 Finite-amplitude instability of parallel shear flows. *J. Fluid Mech.* **27**, 465.

STEWARTSON, K. & STUART, J. T. 1971 A non-linear instability theory for a wave system in plane Poiseuille flow. *J. Fluid Mech.* **48**, 529.

STRUMOLO, G. S. 1978 Perturbed bifurcation theory for plane Poiseuille flow. Ph.D. thesis, Courant Institute of Mathematical Sciences, N.Y.U., N.Y.

STRUMOLO, G. S. & REISS, E. L. 1981 Poiseuille channel flow with driven walls. (Unpublished.)

STUART, J. T. 1960 On the non-linear mechanics of wave disturbances in stable and unstable parallel flows. Part 1. The basic behaviour in plane Poiseuille flow. *J. Fluid Mech.* **9**, 353.

SUBBOTIN, V. I. 1978 Flow in pipes with regular, artificially-produced wall roughness. *Fluid Mech.–Sov. Res.* **7**.

WATSON, J. 1960 On the non-linear mechanics of wave disturbances in stable and unstable parallel flows. Part 2. The development of a solution for plane Couette flow. *J. Fluid Mech.* **14**, 336.

WYGNANSKI, I. J. & CHAMPAGNE, F. H. 1973 On transition in a pipe. Part 1. The origins of puffs and slugs and the flow in a turbulent slug. *J. Fluid Mech.* **59**, 281.